

---

# PEPEVOLVE: POSITION-AWARE DYNAMIC PEPTIDE OPTIMIZATION VIA GROUP-RELATIVE ADVANTAGE

---

Trieu Nguyen<sup>1,2</sup> Hao-Wei Pang<sup>1</sup> Shasha Feng<sup>1</sup>

<sup>1</sup>Merck & Co., Inc., Rahway, NJ, USA

<sup>2</sup>University of South Florida, FL, USA

nguyent368@usf.edu, hao-wei.pang@merck.com, shasha.feng@merck.com

## ABSTRACT

Macrocytic peptides are an emerging modality that combines biologics-like affinity with small-molecule-like developability, but their vast combinatorial space and multi-parameter objectives make lead optimization slow and challenging. Prior generative approaches (e.g., PepINVENT) require chemists to pre-specify mutable positions for optimization, choices that are not always known a priori, and rely on static pretraining and optimization algorithms that limit the model’s ability to generalize and effectively optimize peptide sequences. We introduce **PepEVOLVE**, a position-aware, dynamic framework that learns both where to edit and how to dynamically optimize peptides for multi-objective improvement. **PepEVOLVE** (i) augments pretraining with dynamic masking and CHUCKLES shifting to improve generalization, (ii) uses a context-free multi-armed bandit router that discovers high-reward residues, and (iii) couples a novel evolving optimization algorithm with group-relative advantage to stabilize reinforcement updates. During *in silico* evaluations, the router policy reliably learns and concentrates probability on chemically meaningful sites that influence the peptide’s properties. On a therapeutically motivated Rev-binding macrocycle benchmark, PepEVOLVE outperformed PepINVENT by reaching higher mean scores ~0.8 vs. ~0.6, achieving best candidates with a score of 0.95 (vs. 0.87), and converging in fewer steps under the task of optimizing permeability and lipophilicity with structural constraints. Overall, PepEVOLVE offers a practical, reproducible path to peptide lead optimization when optimal edit sites are unknown, enabling more efficient exploration and improving design quality across multiple objectives.

## 1 Introduction

### 1.1 Challenges in peptide drug discovery and design

Macrocytic peptides sit uniquely between large protein biologics and small molecules [1, 2]. They can deliver biologics-like affinity and engage shallow, flat, or protein–protein interaction interfaces that are often inaccessible to small molecules, while offering a more favorable path to oral delivery than protein therapeutics [1]. Advances in solid-phase peptide synthesis and modular chemistries have increased throughput of peptide drug discovery cycles, and the growing availability of non-canonical amino acids (NCAAs) further expands design flexibility—combining small-molecule-style tunability with peptide-like long-range modularity and structure [3, 4]. Thus, cyclic peptides extend small molecule research beyond the rule of five, while offering a mode similar to biologics, including therapeutic proteins and antibodies. Cyclic peptides have been developed to treat diseases ranging from infectious diseases to cancer and obesity [5, 6]. Akin to oral administration of small molecules, which offer improved safety and patient compliance [7, 8], oral macrocytic peptides offer an attractive modality compared with biologics and small molecule modalities [9]. Recently, several oral macrocytic peptides have advanced clinically, including MSD’s PCSK9 inhibitor MK-0616 [10], Chugai’s Paluratide (LUNA18) pan-KRAS inhibitor [11], and BMS’s PD-L1 inhibitor BMS-986238 [12].

The versatility comes with a challenge: an enormous, combinatorial design space coupled to multi-parameter objectives. A typical 12-mer macrocycle drawn from a library of 4000 monomers yields  $4000^{12}$  candidates. Medicinal chemistry optimization must navigate potency, solubility, permeability, and pharmacokinetics simultaneously, making the mapping

from chemical space to multiparameter optimization (MPO) space highly non-linear. Even when trial-and-error yields compounds meeting target criteria, it is difficult to know whether local structure–activity relationships (SAR) have been exhausted or whether easy-to-make superior neighbors remain unexplored, with consequences for intellectual property. Machine learning (ML) can accelerate exploration of reachable, synthesizable regions of this vast space.

A straightforward ML strategy is *enumerate-and-score*: generate peptide libraries from a chosen monomer set and rank candidates with predictive models. However, enumeration has two practical limitations: one is library dependence, as the searches are bounded by the chosen monomers (e.g., vendor catalogs or in-house sets). If an optimal residue lies just outside this space—such as a subtle ring decoration—the enumerator cannot propose it. The other challenge is that the combinatorial explosion remains prohibitive: even restricting to the “top 20” monomers per position for a 12-mer yields roughly  $4.1 \times 10^{15}$  combinations, quickly overwhelming scoring engines. Moreover, interdependencies across positions mean that the globally optimal combination may require residues not individually ranked in the “top 20” at any single position.

Generative models address these issues by proposing modifications beyond available libraries and, when coupled to reinforcement learning or other optimizers, can navigate MPO landscapes efficiently.

## 1.2 Overview of generative models in peptide design

Generative models have emerged as powerful tools to design novel peptides with desired properties, offering a data-driven solution to overcome the combinatorial bottlenecks in peptide discovery described above [13]. By learning the underlying statistical and chemical patterns of peptide sequences, these models can generate new candidates *de novo* or iteratively optimize existing ones, thereby bridging the gap between vast theoretical design spaces and experimentally tractable discovery.

Such models can be categorized based on their architectures, including variational autoencoders (VAEs) [14, 15], generative adversarial networks (GANs) [16], recurrent neural networks (RNNs) and long short-term memory (LSTM) networks, diffusion models [17], as well as transformer-based [18, 19], and large language models [20, 21, 22, 23, 24]. Early generative models primarily focused on producing peptide sequences composed of natural amino acids, often represented in the FASTA format, such as PepGenWL [23] and Peptide-GPT [22]. These models operate at the residue level and use natural amino acids as building blocks. Recent developments such as PepINVENT [19], PepTune [20], PepThink-R1 [24], HELM-GPT [21] have widened the accessible design space to include non-canonical amino acids (NCAAs), made possible by the increasing availability of NCAA datasets and by architectures capable of encoding atom-level information and proposing atom-level modifications.

Growing interest in macrocyclic peptides has prompted the generative modeling community to develop from sequence-level design into three-dimensional structure-based *de novo* design. For example, AfCycDesign [25] starts from a random cyclic peptide sequence, leverages AlphaFold2 (AF2) [26] to predict its structure, and iteratively optimizes the sequence to match a target structure. BindCraft [27] generates both the backbone and the sequence of a binder using AF2 multimer [28] and optimizes it using MPNN<sub>sol</sub> [29, 30], which is the ProteinMPNN [17] trained on a dataset of only soluble proteins. BoltzGen [17] unifies target protein structure prediction and generative design with an all-atom diffusion framework and allows user-specified binding site constraints for generating protein and peptide binders. Even though these 3D generative approaches for peptide discovery remain limited to canonical amino acids, they serve as novel starting points for hit generation in macrocyclic peptide drug development.

The focus of this work is on lead optimization, using generative models to guide optimization toward desired property ranges, after getting a hit molecule. While *de novo* design can inspire out-of-the-box discovery during early hit identification, property-biased generative models are particularly valuable in lead optimization, where fine-grained control over specific residues is essential. These models typically integrate three components: a generator, a property predictor, and an optimizer. Algorithms such as reinforcement learning [19], genetic algorithms [13], and Monte Carlo Tree Search [20] are commonly employed as optimizers for peptide multi-parameter optimization. Genetic algorithms [13] and Monte Carlo Tree Search [31, 32] are used during inference to guide generation toward specific subspaces, while reinforcement learning directly fine-tunes the prior model into an agent specialized for the desired sequence space.

## 1.3 PepINVENT background and limitations

Among the generative models aimed at property optimization, PepINVENT stands out as a tool that maintains monomer-level modularity and mimics medicinal chemistry design strategies. PepINVENT is a transformer-based generative framework for peptide design that integrates CHUCKLES [33], a SMILES-like representation enabling atom-level control over both natural and non-natural amino acids, while still maintaining the monomer-level boundary. As a result,

chemists can specify the positions they want to keep that may have steep SAR (structure-activity relationships) or are important for binding affinity, while focusing on optimizing the rest of the positions that are amenable to property modulation. In the PepINVENT work, the authors coupled masked-token pretraining with reinforcement learning to optimize physicochemical properties such as permeability and lipophilicity [19].

Despite its effectiveness in property-biased generation, PepINVENT operates under several static assumptions. It requires chemists to pre-define which residues can be modified, a constraint that depends on prior structural knowledge and may overlook key positions. Its pretraining masks a fixed subset of residues, limiting exposure to diverse sequence contexts, and the optimization phase treats the input peptide as static, preventing the model from learning dynamically from its own improved outputs.

These limitations restrict generalization and flexibility, especially when optimal modification sites are unknown. PepEVOLVE builds on this foundation by introducing a new dynamic pretraining approach, automatic position discovery, and a novel evolving algorithm.

## 1.4 Summary of contributions

In this work, we introduce new approaches to both the pretraining and optimization phases. During pretraining, we implement dynamic masking and CHUCKLES shifting to enable the model to learn richer and more comprehensive representations of peptides, ultimately improving its ability to generalize to unseen peptide sequences. We also introduce a context-free multi-armed bandit router that adaptively identifies high-impact residues for editing without requiring chemists to pre-specify mutable positions. In the optimization phase, we propose a novel evolving algorithm that allows PepEVOLVE to learn from a broader range of inputs and contextual variations, rather than relying on a fixed input set as in PepINVENT. Furthermore, we incorporate a group-relative advantage mechanism that enhances learning stability and encourages more effective exploration of the peptide design space, leading to more diverse and higher-quality peptide candidates.

## 2 Methods

### 2.1 Motivation for PepEVOLVE

**Pretraining Phase.** In PepINVENT, the pretraining process relies on a fixed masking dataset, meaning the masked positions in peptide sequences remain the same over training steps. This static setup limits the diversity of learning signals available to the model and increases the risk of overfitting. Since the model repeatedly encounters the same masked positions, it tends to memorize more than generalize, which weakens its performance on unseen peptide sequences. This issue is further compounded for cyclic peptides, which can be converted into multiple linear CHUCKLES representations depending on the chosen starting monomer; training with such a static and fixed sequence dataset can therefore further limit the model’s ability to generalize.

**Optimization Phase.** During optimization with reinforcement learning, PepINVENT keeps the input peptide sequence fixed across all iterations. This restriction prevents the encoder from learning effectively from variations in the input, and the model operates as if it has only a single input state, which limits its capacity to explore and adapt. We hypothesized that it is more effective to allow the peptide to change dynamically during optimization, letting it “evolve” by replacing the current input with improved peptides generated by the model itself. This approach enables the model to iteratively refine peptide sequences and explore the sequence space more effectively. However, the current implementation of PepINVENT limits such evolution. Even when the input sequence is updated with better residues during one of the reinforcement learning steps, the model still processes the sequence as if the evolved positions were masked, which prevents it from fully learning from the updated input.

To overcome these limitations in both phases, PepEVOLVE introduces a dynamic learning framework, leveraging dynamic masking and CHUCKLES shifting during pretraining, and an optimization strategy that enables peptides to iteratively evolve, allowing the model to learn, adapt, and generalize more effectively across a diverse peptide sequence space.

### 2.2 Model Architecture

Our generative framework employs the same implementation and parameter configuration as the transformer architecture introduced in PepINVENT. This transformer model follows an encoder–decoder design and can be formally expressed as a function  $f_{\theta}$ , parameterized by a set of learnable parameters  $\theta$ :

$$f_{\theta} : \chi \times \chi \rightarrow [0, 1]^{|V|} \quad (1)$$

Both the masked peptide sequence  $\tilde{p}$  (source) and the output peptide sequence  $\hat{p}$  (target) are tokenized using a SMILES-based tokenizer, converting them into discrete token sequences that serve as inputs to the encoder and decoder during training. The vocabulary  $V$  represents the complete set of possible tokens within the chemical space  $\chi$ . The function  $f_{\theta}$  defines a probability distribution over the vocabulary  $V$ , learning the likelihood of each token’s occurrence given the preceding context and thus capturing the statistical structure of peptide sequences.

Model parameters are optimized by minimizing the negative log-likelihood (NLL) loss, defined as:

$$\text{NLL}(\tilde{p}, \hat{p}) = - \sum_{t=1}^T \log f_{\theta}(\tilde{p}, \hat{p}_{0:t-1})[\hat{p}_t] \quad (2)$$

Here,  $\tilde{p}$  and  $\hat{p}$  denote the source and target token sequences, respectively, and  $T$  represents the target sequence length. The notation  $[\hat{p}_t]$  refers to the index of the  $t$ -th token  $\hat{p}$ . The model  $f_{\theta}$  estimates the conditional probability of generating the token  $\hat{p}_t$  given all preceding tokens  $\hat{p}_{0,\dots,t-1}$  and the input sequence  $\tilde{p}$ . This probabilistic formulation allows the transformer to capture complex dependencies within the sequence data, facilitating the generation of chemically valid peptide structures.

## 2.3 Pretraining

Our pretraining objective is to equip the generative model with residue-level chemical understanding while remaining robust to representational shifts that arise from multiple linear representations of the same peptide. We build on PepINVENT’s framework and retain its chemically grounded CHUCKLES encoding but modify the masking and sequence presentation, so the model learns context-aware peptide representations rather than memorizing static token patterns.

### 2.3.1 Pretraining Data

A semi-synthetic peptide dataset from PepINVENT was used for model training and validation. The training and validation subsets contained approximately 900,000 and 50,000 peptide sequences, respectively. Each peptide was synthetically assembled from a combination of natural and non-natural alpha-amino acids, the latter derived from a virtual library developed by Amarasinghe et al. [34] through reaction-based enumeration of eMolecules building blocks [34]. To increase chemical diversity, the dataset incorporated randomized stereochemical modifications, N-methylations, and both cyclic and linear topologies, resulting in a chemically diverse yet synthetically tractable peptide space.

Peptide structures were encoded using the CHUCKLES representation, a chemically standardized SMILES-based format that preserves atomic-level detail. In this representation, each monomer follows a consistent N-to-C orientation, beginning at the amino group and extending through the alpha-carbon, sidechain, and backbone, and ending at the carbonyl group. Individual monomers are separated by a vertical bar (“|”), which serves as an explicit boundary marker between residues while preserving the syntactic validity of the concatenated SMILES string. Sequential concatenation of these CHUCKLES segments yields a chemically coherent, fully atomistic SMILES representation of the entire peptide. This encoding ensures atomic-level accuracy across both natural and non-natural amino acid residues and enables the model to learn true chemical connectivity between residues rather than only token-level representations.

Further dataset construction details are provided in Geylan et al [19]. In summary, the final dataset includes peptides ranging from 6 to 18 residues in length, encompassing both linear and macrocyclic topologies. Approximately 30% of residues were replaced with non-natural amino acids to introduce chemical diversity while maintaining synthetic accessibility. The dataset consists of about 40% linear sequences and equal proportions (20% each) of head-to-tail, sidechain-to-tail, and disulfide-bridged macrocycles. Stratified partitioning preserved uniform distributions of sequence length and topology across data splits. Therefore, this is a dataset that is both chemically accessible and relevant to drug discovery.

### 2.3.2 Number of masked positions

During pretraining, PepINVENT uses a BERT-inspired text-infilling [35] objective, where 30% of amino acids in each peptide sequence are randomly masked. This objective trains the model to reconstruct the masked monomers, thereby learning peptide chemistry at the amino acid level. Because the shortest peptides in the pretraining data contained six monomers, a 30% masking ratio always resulted in more than one masked monomer per sequence.

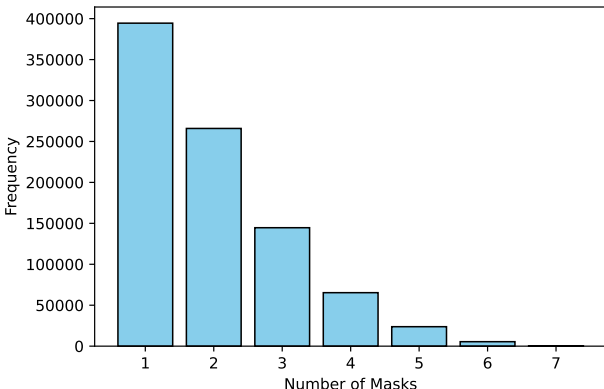


Figure 1: **Sampling distribution for pretraining masks.** Histogram of the number of masked residue positions  $n_{\text{mask}}$  produced by PepEVOLVE’s triangular sampling during pretraining. This ensures that the generative model is adept at generating single-residue mutations.

In PepEVOLVE, we introduced a modified masking strategy to better align with the needs of our downstream optimization framework, where each agent must effectively handle single-residue optimization. The number of masked positions,  $n_{\text{mask}}$ , was sampled from a triangular distribution designed to bias the process toward single-site masking:

$$n_{\text{mask}} = \text{round}(T(a, b, c)) = \text{round}(T(1, 0.4L, 0)), \quad (3)$$

where  $L$  denotes the peptide length, and  $T(a, b, c)$  represents a triangular distribution with lower bound  $a$ , upper bound  $b$ , and mode  $c$  (Figure 1). We set the lower bound to  $a = 1$  and the mode to  $c = 0$  to ensure the peak of the triangular distribution lands at one mask. We also apply rounding to maintain stochastic variability while emphasizing the single-residue optimization task.

### 2.3.3 Dynamic pretraining strategy

Building on the PepINVENT pretraining framework, PepEVOLVE introduces an enhanced text-infilling objective that integrates dynamic masking and CHUCKLES shifting to advance contextual learning and chemical robustness. In contrast to the fixed masking configuration employed by PepINVENT, PepEVOLVE implements dynamic resampling of masked positions at each epoch. This continual resampling exposes the model to a diverse array of context-mask combinations throughout training, thereby mitigating overfitting to specific residue locations and improving generalization of residue-level chemical relationships across variable local environments.

The CHUCKLES shifting mechanism further treats each peptide as a continuous chemical cycle rather than a fixed linear chain (Figure 2). Because cyclic peptides form closed loops without a defined start or end, their structural representation remains invariant under rotational shifts. Randomly shifting the CHUCKLES sequence thus enables the model to learn chemically equivalent representations of the same cyclic peptide, emphasizing intrinsic chemical connectivity rather than positional token order. For linear peptides, CHUCKLES shifting additionally serves as a data augmentation strategy, enhancing the model’s ability to generalize across sequence variations.

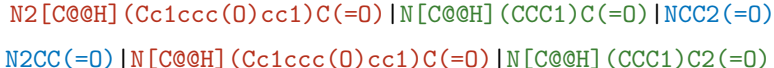


Figure 2: **A toy example of CHUCKLES shifting.** Two different CHUCKLES of the same cyclic peptides are shown. The second sequence is shifted one position to the right, illustrating rotational invariance for cyclic peptides.

To evaluate the performance of this pretraining strategy, the validation dataset was preprocessed in two ways:

- (i) a standard masked set, retaining the original sequences; and
- (ii) a shifted masked set, in which CHUCKLES shifting was applied prior to masking.

Models trained using static masking, as in PepINVENT, performed well on the standard set but exhibited a marked increase in validation loss on the shifted set, indicating sensitivity to positional ordering. Incorporating dynamic masking alone still does not alleviate this issue; the improvement in mean loss is small and still lies within the error bar of the static-masking baseline. In contrast, the combined application of dynamic masking and CHUCKLES shifting yields stable loss across both evaluation subsets, confirming that the model captures the underlying chemical principles governing peptide structure rather than memorizing sequence positions (Figure 3).

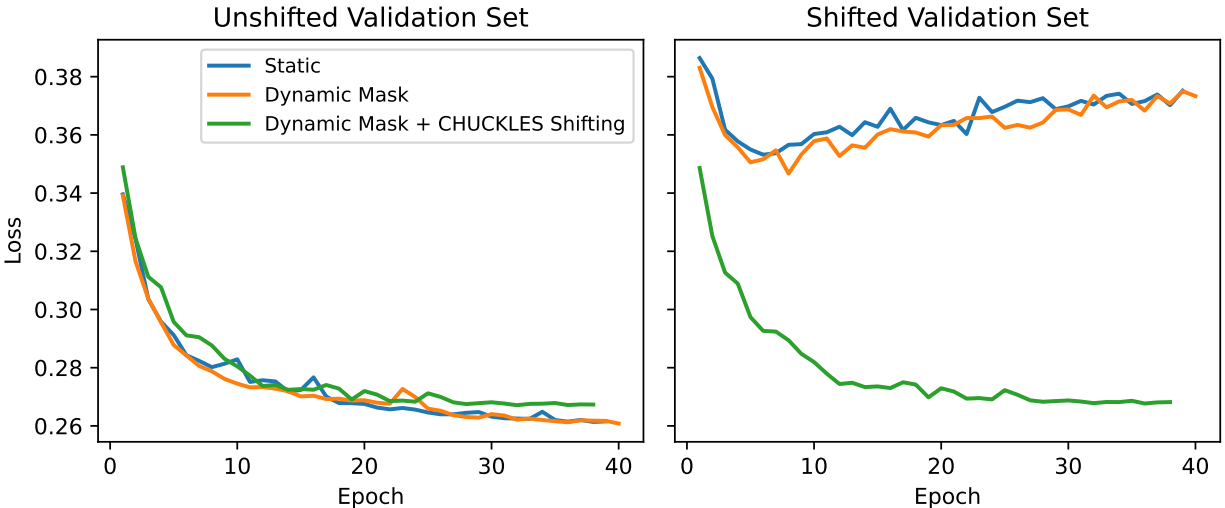


Figure 3: Validation loss for three pretraining strategies: static masking, dynamic masking, and dynamic masking + dynamic CHUCKLES shifting. Left: evaluation on unshifted (standard) sequences. Right: evaluation on CHUCKLES-shifted sequences.

## 2.4 Router Policy for Optimal Residue Identification

As discussed earlier, it is a challenging task for chemists to know which residues are most promising for optimization a priori. To automate this decision, PepEVOLVE introduces a router policy  $\pi$ , a high-level controller that governs the actions of the lower-level agent  $f$ . The router is formulated as a context-free multi-armed bandit that learns to prioritize residues solely from reward feedback of the peptides generated from the agent  $f$ , without conditioning on the peptide sequence.

Formally, a peptide CHUCKLES with  $L$  residues can be represented as

$$p = \text{"r}_1 | \text{r}_2 | \dots | \text{r}_L \text{"} \quad (4)$$

where each  $\text{r}_i$  corresponds to the residue at position  $i$ . Following the PepINVENT framework, the agent  $f$  requires explicit specification of the positions to be optimized, and this is achieved by introducing a special mask token, denoted "?". For subsequent use, we define a masking operator  $M(p, I)$ , which replaces residues at the selected index set  $I \subseteq [L]$  with the token "?", thereby indicating the positions targeted for optimization.

$$M(p, I)[i] = \begin{cases} ?, & \text{if } i \in I, \\ \text{r}_i, & \text{otherwise.} \end{cases} \quad (5)$$

The router policy is parameterized by  $L$  variables, each indicating the probability of selecting a particular residue position within a categorical distribution, expressed as  $\pi_\theta$  where  $\theta \in \mathbb{R}^L$ . During each routing step, the policy samples a batch  $B$  of  $K$  unique position indices to be optimized; these positions represent the subset of residues that is potentially optimal for modification. Each sampled subset is drawn from the categorical distribution governed by  $\pi_\theta$  as follows:

$$[I]_{\{B \times K\}} = [i_{\{bk\}}]_{\{B \times K\}} \sim \pi_\theta, \quad I \in [L]^{\{B \times K\}}, \quad (6)$$

$$I_b = (i_{\{b1\}}, \dots, i_{\{bK\}}) \in [L]^K. \quad (7)$$

For each selected subset  $I_b$ , a masked peptide  $\tilde{p}_{I_b} = M(p, I_b)$  is created and is then input into the shared agent  $f$  to generate  $G$  candidate peptides:

$$\{\hat{p}_{I_b}^g\}_{g=1}^G \sim f(\tilde{p}_{I_b}). \quad (8)$$

Each of these candidates receives an individual scalar reward  $R_{I_b}^g$ , and the mean reward across the  $G$  candidates serves as the aggregate performance measure for the sampled subset:

$$\bar{R}_{I_b} = \frac{1}{G} \sum_{g=1}^G R_{I_b}^g. \quad (9)$$

This hierarchical design distributes control between two complementary levels. The router acts as a high-level controller, learning which residues are most valuable to modify. The optimizing agent operates at a lower level, performing the actual modifications at the selected positions and learning which specific changes yield the greatest improvement in reward. Together, this coordination enables PepEVOLVE to efficiently explore both where and how to modify peptides for optimal outcomes.

### Router Update

The router policy is updated via a policy-gradient objective that leverages the aggregate rewards  $R_{I_b}$  obtained for each sampled subset of positions [36]. Specifically, the update follows a REINFORCE-style [36] gradient estimator with the addition of an adaptive baseline to reduce variance. Given a batch of  $B$  sampled subsets and their corresponding scores  $R_{I_b}$ , the advantage for each sample is computed as

$$A_{I_b} = \bar{R}_{I_b} - \mathbb{E}[R_{I_b}], \quad (10)$$

where the expectation is approximated by a running exponential average, forming a moving baseline that stabilizes training. This baseline  $\mathbb{E}[R_{I_b}]$  is updated after each step according to

$$\text{baseline} \leftarrow \lambda \text{baseline} + (1 - \lambda) \frac{1}{B} \sum_b R_{I_b}, \quad (11)$$

where  $\lambda \in [0, 1)$  is the baseline smoothing coefficient.

The router assigns a log-probability to each sampled mask  $I_b$  through its categorical distribution,  $\log \pi_\theta(I_b)$ . The policy gradient (PG) loss is then expressed as

$$\mathcal{L}_{\text{PG}} = -\frac{1}{B} \sum_b A_{I_b} \log \pi_\theta(I_b), \quad (12)$$

encouraging the router to increase the likelihood of residue subsets yielding higher-than-expected rewards.

To maintain exploration and prevent premature convergence, an entropy regularization term is additionally incorporated. The router’s entropy  $\mathcal{H}(\pi_\theta)$  quantifies its uncertainty over positions, promoting diversity in selected mutation sites. The final loss combines the policy gradient and entropy terms:

$$\mathcal{L}_{\text{router}} = \mathcal{L}_{\text{PG}} - \beta \mathcal{H}(\pi_\theta), \quad (13)$$

where the coefficient  $\beta$  controls the degree of entropy regularization. To gradually shift from exploration to exploitation,  $\beta$  is annealed linearly over training steps from an initial value  $\beta_{\text{start}}$  to a final value  $\beta_{\text{end}}$ .

In summary, this update scheme allows the router to continually refine its probabilistic focus, allocating higher selection probabilities to residue positions that have historically yielded stronger downstream improvements. The combination of advantage normalization, entropy annealing, and baseline correction ensures a stable yet adaptive learning process that balances exploration of new mutation sites with exploitation of high-performing regions.

## 2.5 Evolving Strategy

Each input context is handled by a different agent. This configuration is advantageous when the output space is heterogeneous, where the relationships between contexts and their optimization dynamics differ significantly. By allowing each agent to specialize in its own context, they can better capture diverse optimization behaviors that would

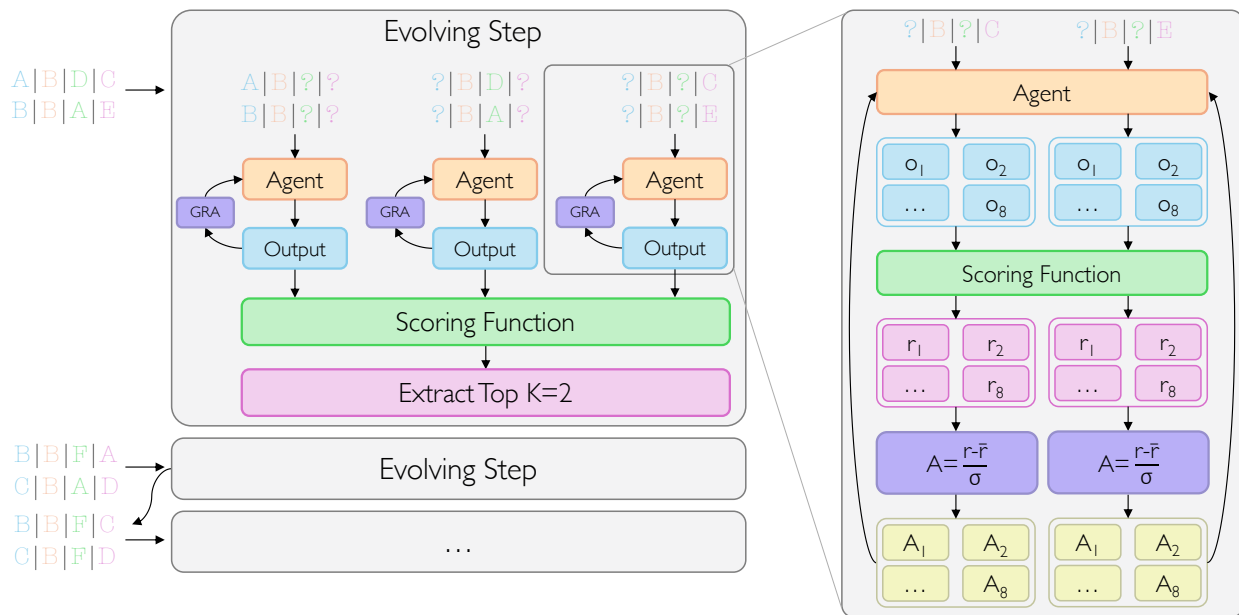


Figure 4: **Evolving phase algorithm with group-relative advantage (GRA)**. Example of neighbor-masking using the input sequence "A|B|C|D" with a set of optimized positions  $O = \{0, 2, 3\}$ . At each step, the top- $K$  peptides (here  $K = 2$ ) from the previous step are selected as seed inputs. For each seed,  $|O| = 3$  input contexts are extracted. In every context,  $G = 8$  candidate sequences are generated per seed, and their rewards are computed and normalized using the group-relative advantage.

otherwise be averaged out in the single-agent setup. Self-mask agent is, in essence, an agent that specializes in a single position, analogous to how individual chemists focus on different residues/positions to optimize. The self-mask agent builds in-depth knowledge about how to optimize a specific position. The neighbor-mask agent is modifying other positions rather than the specified position; this is analogous to adjusting multiple positions together to drive properties into an optimal region.

To illustrate how these masking strategies and modes work in practice, a detailed example demonstrating both self-mask and neighbor-mask configurations for a toy peptide sequence is provided in the Supplementary Information (Section S1). For each input peptide  $\tilde{p}^j$ ,  $G$  candidate peptides  $\hat{p}_g^j$  are generated. The candidates generated from each input peptide  $\tilde{p}^j$  form a group, within which rewards are computed using a group-relative advantage mechanism. To update the agent, the relative advantage of each candidate within its group is computed as:

$$A_g^j = \frac{R(\hat{p}_g^j) - \bar{R}^j}{\sigma_R^j + \varepsilon} \quad (14)$$

Here,  $\bar{R}^j$  denotes the mean reward of all candidate peptides generated from the same seed  $\tilde{p}^j$ , representing the average performance within the group, and  $\sigma_R^j$  represents the standard deviation of rewards within that group, which normalizes the advantage values to ensure scale invariance and stabilize learning across different reward magnitudes and  $\varepsilon$  is a small constant added for numerical stability. This enables learning to focus on the relative quality of candidates derived from the same seed peptide. Rather than comparing all candidates globally, each group formed from a common seed functions as an independent reference frame. Within a group, candidates are evaluated based on how much better or worse they perform compared to their peers. Normalizing performance within each group provides a balanced and stable learning signal, ensuring that updates emphasize consistent improvement among all seeds.

To demonstrate the process, as illustrated in Figure 4, an example with the input peptide sequence "A|B|C|D", together with neighbor-mask context visibility, a set of optimal positions  $O = \{0, 2, 3\}$ , evolution parameters (top number of seed  $K = 2$  and number of candidates  $G = 8$ ) is set to be optimized.

At the initial step (step 0), which is not shown in the figure,  $K = 2$  peptides are initialized from the model with the input "?|B|?|?" producing the seed inputs "A|B|D|C" and "B|B|A|E". Because there are  $|O| = 3$  target positions to

optimize, three distinct input contexts are defined, each processed sequentially by the agent. For every context, the agent handles  $K = 2$  CHUCKLES, and for each CHUCKLES, the agent generates  $G = 8$  outputs. These outputs are scored and normalized using the group-relative advantage (GRA) method. The resulting advantage values are then used to update the agent’s weights, progressively refining its policy and performance.

After all peptides from the three contexts are generated, they are aggregated into a single pool and re-evaluated using similar scoring functions to get the raw scores, this time without normalization by GRA. From this pool, the top  $K = 2$  peptides are selected based on their computed scores to become new seed inputs for the next step of the evolving phase. This procedure continues iteratively, following the same algorithm throughout the entire evolving process.

By continuously exposing the model to a variety of inputs and contexts at every step, our evolving algorithm enables learning from a richer and more diverse input space. GRA plays a central role by guiding the model toward identifying which actions yield the greatest improvement. This iterative exposure and feedback allow the model to progressively refine its decision-making and improve performance throughout the evolving phase.

### 3 Results

#### 3.1 Evaluating router effectiveness in identifying optimal residues

To evaluate the effectiveness of the router policy, we conducted experiments on three distinct test cases, each defined by an objective function of increasing complexity. The analysis focused on the learned probability distribution of the policy across all residue positions.

##### 3.1.1 Hydrogen bond donor decrease

In this test case, we synthetically created a peptide and arbitrarily placed two special amino acids at positions **13** and **15** (Figure 5-A)

**Position 13:** N[C@@H](CN[C@@H]CN[C@@H]C(=O)N)C(=O), containing 4 hydrogen bond donors

**Position 15:** N[C@@H]N[C@@H](Cc1c[nH]c2ccccc12)C(=O), containing 3 hydrogen bond donors

To evaluate the routing policy’s performance, besides the two amino acids above, other amino acids in the peptide only had 1–2 hydrogen bond donors, and the objective function was defined to minimize the total number of hydrogen bond donors within the peptide. Therefore, the ground truth for the top optimal position was position 13, and the second optimal position was position 15. We examined two scenarios: (1) identifying a single most optimal position and (2) identifying two most optimal positions.

In the single-position scenario, the routing policy successfully converged on position 13, with the probability distribution approaching 1.0 over time, indicating a strong preference for that site as the optimal choice. In the two-position scenario, the policy effectively distributed probability between positions 13 and 15. Both were correctly identified as optimal sites, with the policy still displaying a slightly stronger preference for position 13, aligning with its higher hydrogen bond donor count.

##### 3.1.2 LogP decrease

In this test case, we used the LUNA18 peptide and focused on two specific amino acids that notably influence the overall LogP value due to their aromatic side chains:

**Position 6:** N(CC)[C@@H](Cc1ccc(C)cc1)C(=O), contributes slightly to an increase in LogP

**Position 8:** N[C@@H](CCc1cc(F)c(C(F)(F)F)c(F)c1)C(=O), contributes most significantly to the LogP increase.

Therefore, to assess the router policy’s performance, the objective is defined as minimizing the overall LogP of the peptide. The ground truth, therefore, corresponds to the two aromatic ring positions. As in the first test, we also evaluate the policy on two scenarios, identifying one and two optimal positions, over 500 routing steps. In the single-position experiment (Figure 6-B), the routing policy rapidly concentrated its probability mass on position 8, with values approaching 1.0 as training progressed. This indicates the model’s strong confidence in selecting position 8 as the most influential contributor to the LogP, consistent with the expected ground truth. When extended to identify two positions (Figure 6-C), the policy distributes its focus across positions 6 and 8. Both were accurately highlighted as key contributors, though position 8 maintains a marginally higher probability, aligning with its greater impact on increasing the peptide’s overall LogP.

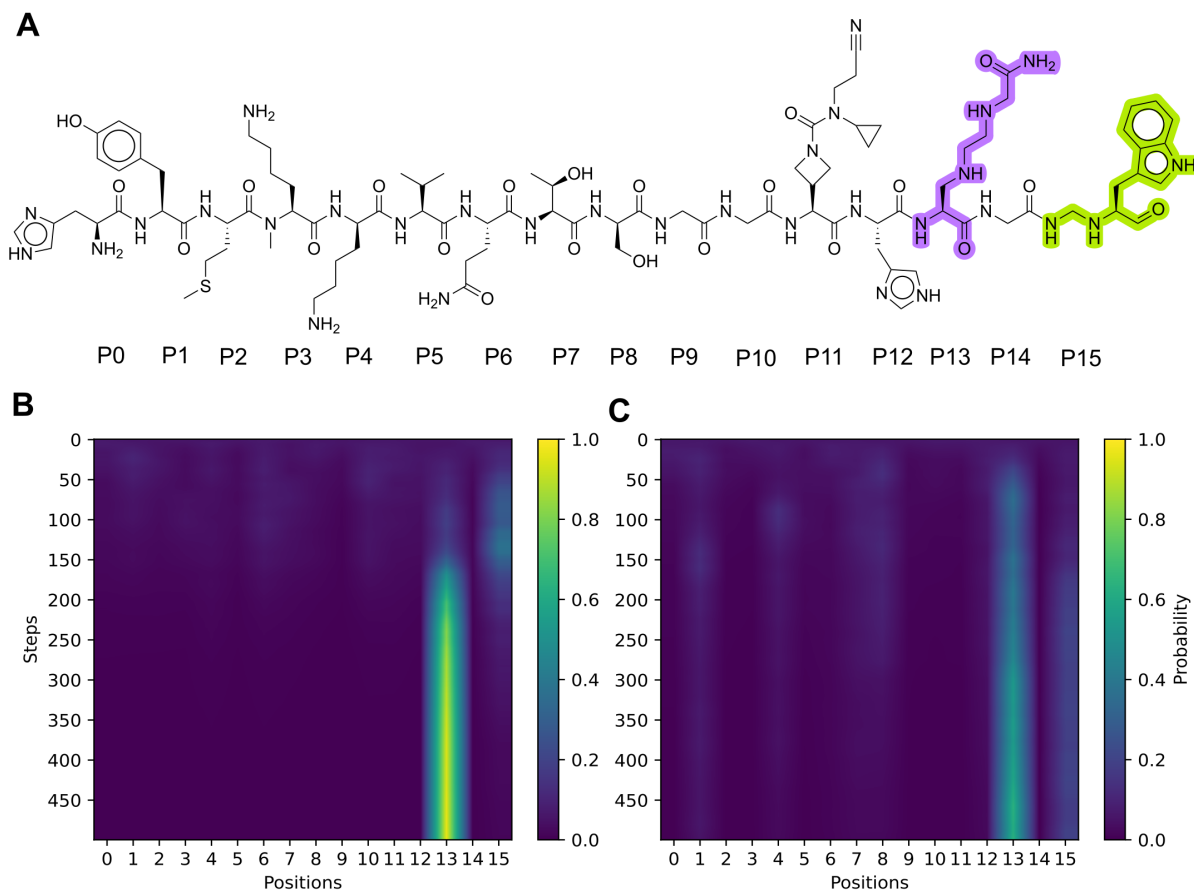


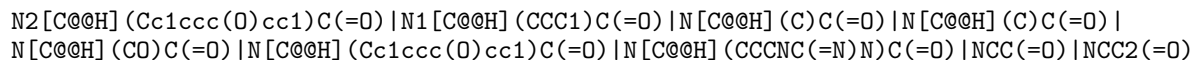
Figure 5: **Router policy convergence for minimizing the number of hydrogen-bond donors.** (A) Router selection probabilities over routing steps when the objective is to minimize the total number of hydrogen-bond donors in a synthetic peptide. (B) Probability of the router identifying one optimal position. (C) Probability of the router identifying two optimal positions.

### 3.1.3 Adversarial task: LogP increase

In this test case, we build upon the previous experiment, which identified the optimal positions for reducing the peptide’s LogP. As the router policy learns these optimal modification sites, the optimizing agent  $f$  is also updated to generate better peptides with lower LogP values. From the resulting set of generated peptides, the one with the lowest LogP is selected, modifying positions 6 and 8. To evaluate the robustness of the router policy, the objective function is reversed, aiming at increasing the peptide’s LogP. The policy is then tasked with finding two optimal positions that would maximize the reward under this new objective. As illustrated in (Figure 7), the router policy successfully converges on positions 6 and 8, precisely matching the known ground truth.

## 3.2 Evaluating optimization capability: PepEVOLVE vs. PepINVENT

To evaluate PepEVOLVE against PepINVENT, both models are benchmarked on the therapeutically relevant Rev-binding peptide (RBP) used in PepINVENT’s original study. Rev is essential in the HIV lifecycle and has been a target for antiviral discovery. The RBP sequence *YPAASYR* was identified as a potential Rev inhibitor [37]. In the work by Wu et al. [38], two glycine residues were appended, and a head-to-tail macrocyclization was performed to yield the macrocycle CHUCKLES:



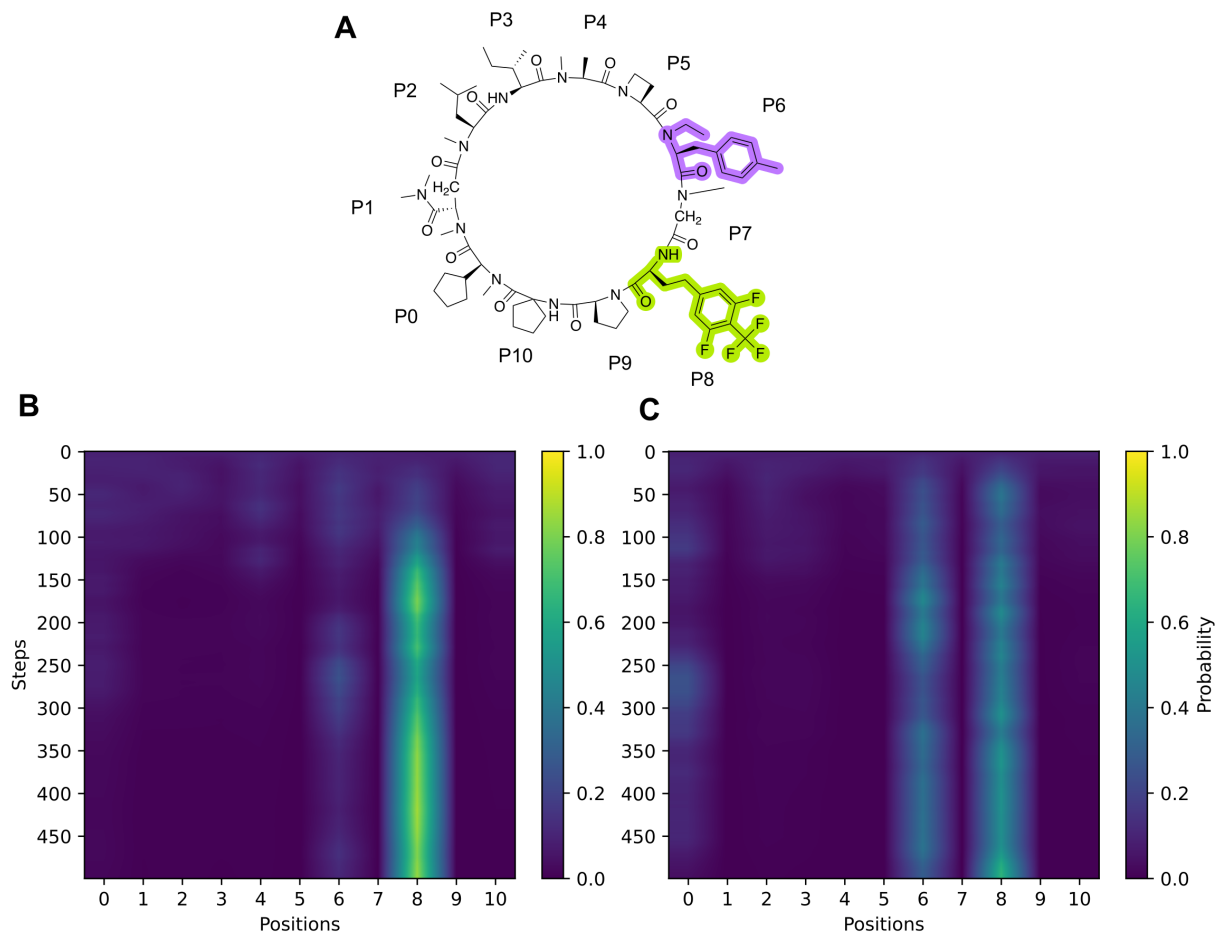


Figure 6: **Router policy convergence for minimizing LogP on LUNA18 peptide.** (A) Router selection probabilities over routing steps when the objective is to lower overall lipophilicity (LogP). (B) Probability of the router identifying one optimal position. (C) Probability of the router identifying two optimal positions.

### 3.2.1 Experiment setup

We evaluate four PepEVOLVE configurations: self-mask single-agent (SS), self-mask multi-agent (SM), neighbor-mask single-agent (NS), and neighbor-mask multi-agent (NM). Because the mutable sites are known, the alanines and the glycines (introduced solely to enable cyclization), routing is bypassed, and direct evolution is performed. Each PepEVOLVE step processes one input context; for this task, there are four target positions. To equalize the total number of update steps across methods, we therefore run PepEVOLVE for 250 steps ( $4 \times 250 = 1000$  context iteration) and PepINVENT for 1000 steps. For the evolving phase, we use  $K = 16$  and  $G = 8$ .

Because the solubility code that was used in PepINVENT is not publicly available, we compare the two models on the accessible scoring components: permeability, maximum ring size, lipophilicity, and custom SMARTS alerts. To emphasize biological relevance, we aggregate scores using a geometric mean while giving higher weight to permeability (exponent = 3), as it is the primary optimization objective. Lipophilicity is targeted around  $-4.0$  to align with the range used in PepINVENT:

$$\text{Score} = (S_{\text{perm}}^3 \times S_{\text{ring}} \times S_{\text{lipophilicity}} \times S_{\text{SMARTS}})^{1/6}. \quad (15)$$

This makes the total scale interpretable while preserving multiplicative penalties when any component scores poorly.

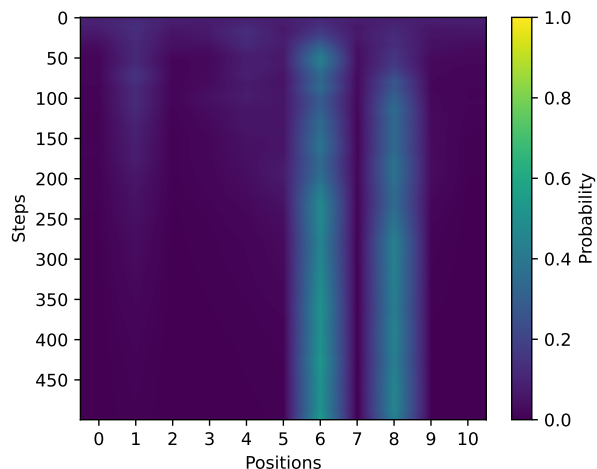


Figure 7: **Router policy convergence for the adversarial test.** Router selection probabilities over routing steps when the objective is reversed to increase LogP of the lowest-LogP peptide extracted from the LUNA18 test case.

### 3.2.2 Scores distribution of generated peptides and optimization dynamics

We summarize the distribution over unique peptides (Figure 8-left) and the mean score of generated peptides over the reinforcement learning steps (Figure 8-right). Across all four configurations, PepEVOLVE clearly outperforms PepINVENT. PepINVENT’s generated peptide scores distribution concentrates around  $\approx 0.6$  with virtually no mass beyond 0.8, and its best generated sequence has a score of  $\approx 0.87$ . In contrast, PepEVOLVE shifts the bulk of the distribution upward: means are  $\approx 0.8$  with heavy tails extending to  $\geq 0.9$ –0.95. Optimization dynamics mirror this: PepEVOLVE reaches high-scoring regions in far fewer steps and maintains higher means throughout. Among PepEVOLVE variants, SS exhibits the fastest early climb (rapidly entering the  $\geq 0.9$  region), SM attains the highest terminal scores, NS tracks closely behind with a stable ascent, and NM lags the others but still surpasses PepINVENT by a wide margin.

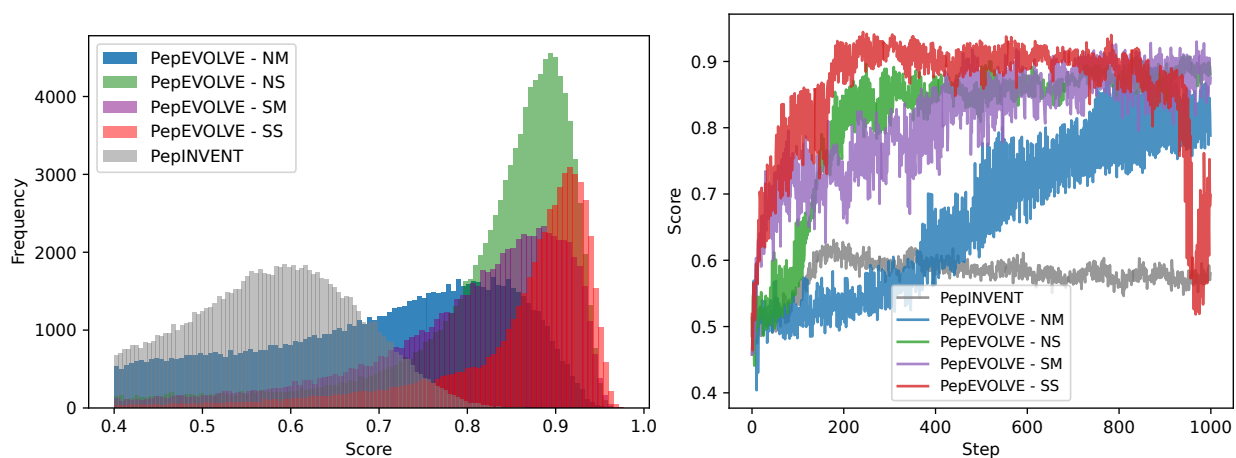


Figure 8: **PepEVOLVE vs. PepINVENT on Rev-binding macrocycle optimization.** Comparison of the scores of generated peptides under permeability-aware multi-objective function (see Eq. 15) between PepINVENT and four PepEVOLVE configurations (neighbor-mask multi-agent, NM; neighbor-mask single-agent, NS; self-mask multi-agent, SM; self-mask single-agent, SS). Left: distribution of generated peptide scores. Right: average generated peptide scores over the reinforcement learning steps.

### 3.2.3 Yield-quality trade-off

To validate the efficiency of generating high-quality peptides, we partitioned the unique peptides into different score bins, as shown in Figure 9. PepINVENT returns many unique sequences, but they are dominated by  $\leq 0.8$  scores. All PepEVOLVE variants shift their mass into the 0.80–0.94 bands, with significant counts above 0.9 bins, which could not be reached by PepINVENT. Notably, NS achieves the largest overall yield, exceeding PepINVENT, while keeping a substantial fraction in the 0.90–0.94 range; SS produces fewer total sequences than NS but the highest proportion in the top bins; SM balances yield and quality; and NM, while generating many sequences, still rebalances markedly toward higher scores relative to PepINVENT. Taken together, PepEVOLVE improves both sample efficiency (fewer steps to high scores) and the quality distribution without sacrificing diversity of unique outputs.

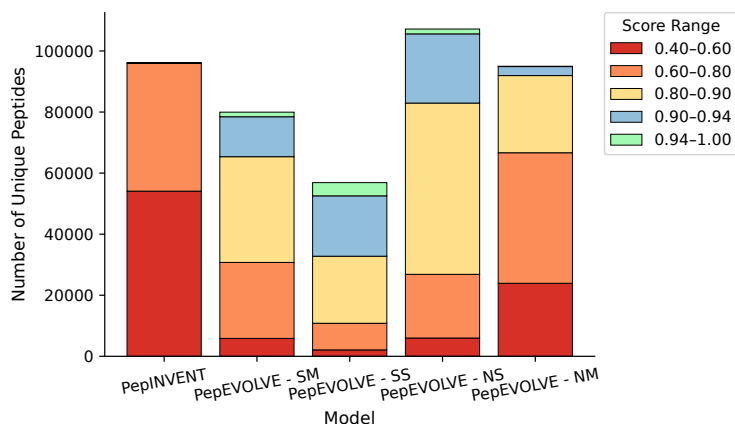


Figure 9: Number of unique peptides by score bins generated by PepINVENT and four PepEVOLVE modes. A higher fraction of peptides with scores 0.8-1.0 was generated in the PepEVOLVE models.

### 3.2.4 Assess top-quality generated peptides

We visualize the peptides to inspect the motifs generated by the models, including the original peptide, PepINVENT top-scoring peptide, and the top representative peptides from the four modes of PepEVOLVE (Figure 10). Using the same number of total steps, PepINVENT generates relatively simple monomers for the four positions, while PepEVOLVE generates more elaborate monomers at these positions. All the models commonly use amide and urea motifs to lower LogP, and use N-methylation to improve permeability. Some PepEVOLVE-generated peptides also explore sulfonamide motifs to optimize towards the desired LogP. Overall, the dynamic optimization in PepEVOLVE allows the model to have more capacity to generate novel and bespoke chemical matter.

### 3.2.5 Summary

Across configurations, PepEVOLVE consistently outperforms PepINVENT: (i) higher mean and best-case scores, (ii) faster convergence to the high-scoring region, and (iii) a favorable yield–quality profile with many more peptides above 0.8 (and sizeable counts above 0.9). These gains hold under a permeability-aware objective and are obtained with fewer effective steps, demonstrating both efficiency and robustness.

Given there are different modes in PepEVOLVE, for practical applications, we recommend choosing the configuration to match your goal and compute budget:

- **Exploration or trend searching.** Start with neighbor-mask, single-agent (NS). It is the most stable across steps, since the single agent oversees all the positions. This yields the largest set of unique peptides and provides consistently strong scores while covering chemical space.
- **Top-hit search.** If the priority is to surface the highest-scoring candidates, start with self-mask single-agent (SS). It reaches the 0.9–1.0 band fastest and produces the highest fraction of elite peptides, at the cost of fewer uniques and a higher risk of late-stage mode collapse.
- **When to use multi-agent.** If scores widely fluctuate, different masking contexts might have significant optimization dynamics, switch to the corresponding multi-agent variants (SM or NM). These capture context-specific dynamics that a single agent may average out.

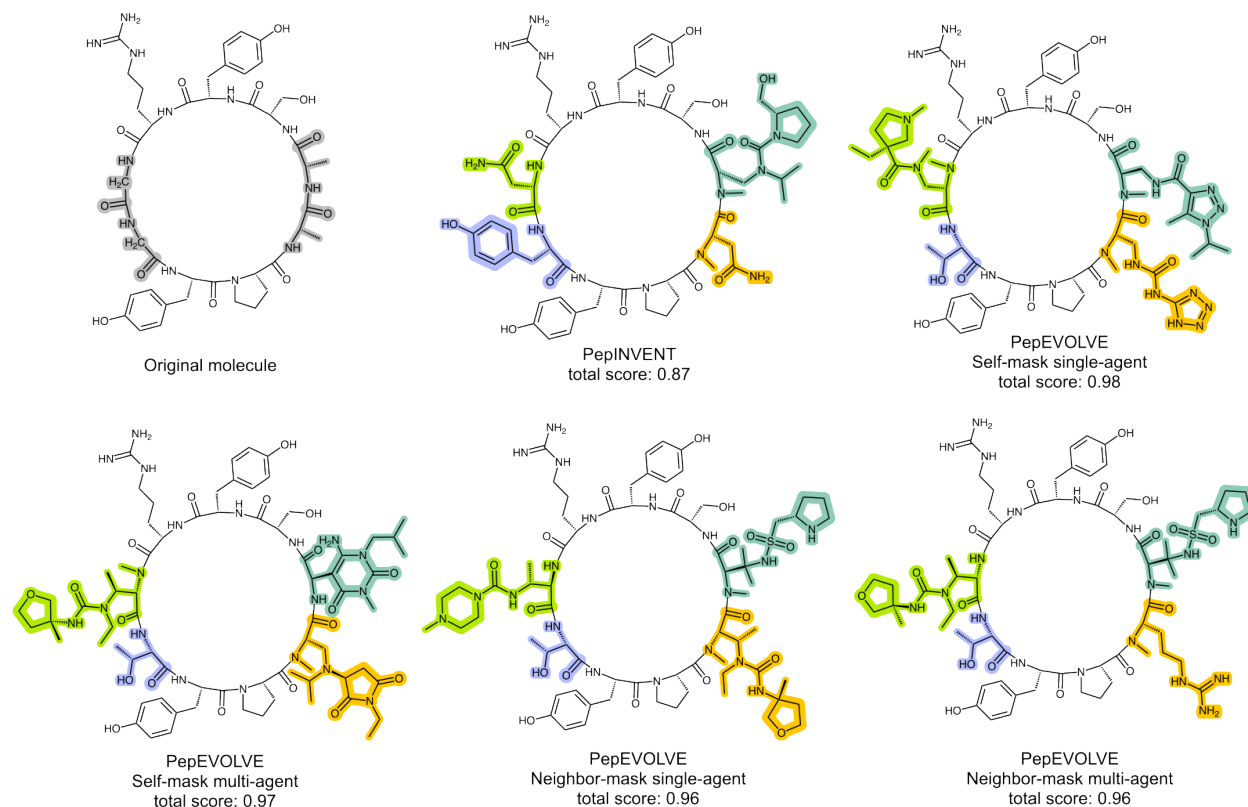


Figure 10: **Visualization of top compounds generated by PepEVOLVE vs. PepINVENT on Rev-binding macrocycle optimization.** PepEVOLVE models generate more complex chemistry entities.

## 4 Discussion

This work introduces PepEVOLVE, a position-aware, dynamic optimization framework that augments a transformer generator with (i) dynamic pretraining (dynamic masking and CHUCKLES shifting), (ii) a router policy to automatically identify high-value residue positions with high probability of success, and (iii) an evolving optimization loop with group-relative advantage (GRA). Collectively, these innovations yield faster convergence and bespoke monomer designs than PepINVENT on a therapeutically motivated benchmark, with mean scores around 0.8 and best designs approaching 0.95 under a permeability-weighted geometric scoring function, while PepINVENT plateaus near 0.8 at best. PepEVOLVE provides a practical path for lead optimization when medicinal chemists either do not know a priori which positions to change or wish to explore broader local neighborhoods efficiently.

Generative peptide design has progressed from residue-level VAEs, GANs, and RNNs to transformer and LLM-based models with NCAA-capable encodings [15, 16, 18, 19, 20, 21, 22, 23, 24]. PepINVENT established property-biased reinforcement learning over CHUCKLES, but requires users to pre-specify mutable positions, which risks missing more influential sites. Multi-agent frameworks (e.g., MultiMol [39], MT-Mol [40]) highlight the value of role specialization in molecular design. PepEVOLVE advances this line by (a) removing static assumptions in pretraining via dynamic masking and rotationally invariant CHUCKLES shifts that stabilize validation loss across shifted/unshifted inputs, and (b) introducing a context-free bandit router that learns where to edit from reward alone, no sequence conditioning or hand-picked sites required.

**Limitations.** Our comparative metric removes solubility due to unavailable code and instead uses a permeability-weighted geometric mean (a weight of 3 for permeability and a weight of 1 for all other objectives) over ring size, lipophilicity, and SMARTS alerts; conclusions therefore reflect the chosen surrogate objective rather than full developability. Benchmarking centers on one public case (Rev-binding macrocycle with predefined mutable A/G positions), with 250 PepEVOLVE steps versus 1000 for PepINVENT to equalize context passes; broader targets and alternative step budgets should be tested. The router is context-free (sequence-agnostic), which may miss sequence-

dependent or 3D-structural contingencies. Finally, group relative advantage, while stabilizing across local groups, can reduce diversity via group-wise normalization pressure.

## 5 Conclusion

PepEVOLVE tackles a core bottleneck in macrocyclic peptide design: deciding where to change a sequence and how to evolve it so multiple properties improve together. By pairing dynamic pretraining (mask resampling and CHUCKLES shifting) with a router that learns high-value positions and an evolving, group-relative advantage optimizer, the framework shifts from static, position-guessed edits to data-driven, position-aware optimization. Across synthetic objectives and the RBP benchmark, PepEVOLVE consistently produced higher-scoring peptides and reached strong solutions in fewer steps than PepINVENT, while the router reliably found the positions most aligned with the objective. This approach closes the loop between medicinal intuition and algorithmic search, it reduces exploration in an enormous design space and makes lead optimization more systematic, transparent, and reproducible, helping advance the state of computational peptide design.

### Acknowledgement

We are grateful to Nicolas Boyer, James P. Jewell, Ed Miller, and Ryan Chau for their chemists' intuition and strategic insights. We thank Peter Zhang, Ruheng Wang, Ruibo Zhang, Yixiang Mao, Alec Glisman, Haote Li, Kenneth López Pérez, and Song Yin for valuable discussions on peptide prediction and generation methodologies. We also acknowledge Sebastian Schneider, Liying Zhang, and Jennifer Johnston for their strategic guidance throughout this project.

### References

- [1] Daniël Leenheer, Peter Ten Dijke, and Christopher John Hipolito. "A current perspective on applications of macrocyclic-peptide-based high-affinity ligands". en. In: *Biopolymers* 106.6 (Nov. 2016), pp. 889–900.
- [2] Alexander A Vinogradov, Yizhen Yin, and Hiroaki Suga. "Macrocyclic peptides as drug candidates: Recent progress and remaining challenges". en. In: *J. Am. Chem. Soc.* 141.10 (Mar. 2019), pp. 4167–4181.
- [3] Teresa A F Cardote and Alessio Ciulli. "Cyclic and macrocyclic peptides as chemical tools to recognise protein surfaces and probe protein-protein interactions". en. In: *ChemMedChem* 11.8 (Apr. 2016), pp. 787–794.
- [4] Antoine Henninot, James C Collins, and John M Nuss. "The current state of peptide drug discovery: Back to the future?" en. In: *J. Med. Chem.* 61.4 (Feb. 2018), pp. 1382–1414.
- [5] Lia Costa, Emília Sousa, and Carla Fernandes. "Cyclic peptides in pipeline: What future for these great molecules?" en. In: *Pharmaceuticals (Basel)* 16.7 (July 2023), p. 996.
- [6] Huiya Zhang and Shiyu Chen. "Cyclic peptide drugs approved in the last two decades (2001-2021)". en. In: *RSC Chem. Biol.* 3.1 (Jan. 2022), pp. 18–31.
- [7] Tsvetelina H Baryakova, Brett H Pogostin, Robert Langer, and Kevin J McHugh. "Overcoming barriers to patient adherence: the case for developing innovative drug delivery systems". en. In: *Nat. Rev. Drug Discov.* 22.5 (May 2023), pp. 387–409.
- [8] Mohammed S Alqahtani, Mohsin Kazi, Mohammad A Alsenaidy, and Muhammad Z Ahmad. "Advances in oral drug delivery". en. In: *Front. Pharmacol.* 12 (Feb. 2021), p. 618411.
- [9] Lei Wang, Nanxi Wang, Wenping Zhang, Xurui Cheng, Zhibin Yan, Gang Shao, Xi Wang, Rui Wang, and Caiyun Fu. "Therapeutic peptides: current applications and future directions". en. In: *Signal Transduct. Target. Ther.* 7.1 (Feb. 2022), p. 48.
- [10] Douglas G. Johns, Puja Banka, Zexun Zhou, Artis Klapara, Fuh-Rong Tsay, Jongrook Kong, Richard J. Varsolona, Richard Desmond, Peter E. Maligres, Melanie Marota, and et al. "Compounds for treating conditions related to PCSK9 activity". WO Patent WO2023023245A1, published Feb 23, 2023. 2022.
- [11] Mikimasa Tanada, Minoru Tamiya, Atsushi Matsuo, Aya Chiyoda, Koji Takano, Toshiya Ito, Machiko Irie, Tomoya Kotake, Ryuichi Takeyama, Hatsuo Kawada, Ryuji Hayashi, Shiho Ishikawa, Kenichi Nomura, Noriyuki Furuichi, Yuya Morita, Mirai Kage, Satoshi Hashimoto, Keiji Nii, Hitoshi Sase, Kazuhiro Ohara, Atsushi Ohta, Shino Kuramoto, Yoshikazu Nishimura, Hitoshi Iikura, and Takuya Shiraishi. "Development of orally bioavailable peptides targeting an intracellular protein: From a hit to a clinical KRAS inhibitor". en. In: *J. Am. Chem. Soc.* 145.30 (Aug. 2023), pp. 16610–16620.
- [12] Patrick M. Scola. *Discovery of BMS-986238, a second-generation macrocyclic peptide inhibitor of programmed death-ligand 1 (PD-L1)*. ACS Spring 2025 meeting presentation (abstract). 2025.
- [13] Fangping Wan, Daphne Kontogiorgos-Heintz, and Cesar de la Fuente-Nunez. "Deep generative models for peptide design". en. In: *Digit. Discov.* 1.3 (June 2022), pp. 195–208.

- [14] Payel Das, Tom Sercu, Kahini Wadhawan, Inkit Padhi, Sebastian Gehrmann, Flaviu Cipcigan, Vijil Chenthamarakshan, Hendrik Strobel, Cicero Dos Santos, Pin-Yu Chen, Yi Yan Yang, Jeremy P K Tan, James Hedrick, Jason Crain, and Aleksandra Mojsilovic. “Accelerated antimicrobial discovery via deep generative models and molecular dynamics simulations”. en. In: *Nat. Biomed. Eng.* 5.6 (June 2021), pp. 613–623.
- [15] Sijie Chen, Tong Lin, Ruchira Basu, Jeremy Ritchey, Shen Wang, Yichuan Luo, Xingcan Li, Dehua Pei, Levent Burak Kara, and Xiaolin Cheng. “Design of target specific peptide inhibitors using generative deep learning and molecular dynamics simulations”. en. In: *Nat. Commun.* 15.1 (Feb. 2024), p. 1611.
- [16] Shraddha Surana, Pooja Arora, Divye Singh, Deepti Sahasrabudde, and Jayaraman Valadi. “PandoraGAN: Generating antiviral peptides using generative adversarial network”. en. In: *SN Comput. Sci.* 4.5 (Aug. 2023).
- [17] Hannes F. Stärk, Felix Faltings, MinGyu Choi, Yuxin Xie, Eunsu Hur, Timothy O’Donnell, Anton Bushuiev, Talip Uçar, Saro Passaro, Weian Mao, Mateo Reveiz, Roman Bushuiev, Tomáš Pluskal, Josef Sivic, Karsten Kreis, Arash Vahdat, Shamayeeta Ray, Jonathan T. Goldstein, Andrew Savinov, Jacob A. Hambalek, Anshika Gupta, Diego A. Taquiri-Diaz, Yaotian Zhang, A. Katherine Hatstat, Angelika Arada, Nam Hyeong Kim, Ethel Tackie-Yarboi, Dylan Boselli, Lee Schnaider, Chang C. Liu, Gene-Wei Li, Denes Hnisz, David M. Sabatini, William F. DeGrado, Jeremy Wohlwend, Gabriele Corso, Regina Barzilay, and Tommi Jaakkola. *BoltzGen: Toward Universal Binder Design*. 2025.
- [18] Sangjeong Lee and Hyunwoo Kim. “Bidirectional de novo peptide sequencing using a transformer model”. en. In: *PLoS Comput. Biol.* 20.2 (Feb. 2024), e1011892.
- [19] Gökçe Geylan, Jon Paul Janet, Alessandro Tibo, Jiazhen He, Atanas Patronov, Mikhail Kabeshov, Werngard Czechtizky, Florian David, Ola Engkvist, and Leonardo De Maria. “PepINVENT: generative peptide design beyond natural amino acids”. en. In: *Chem. Sci.* 16.20 (May 2025), pp. 8682–8696.
- [20] Sophia Tang, Yinuo Zhang, and Pranam Chatterjee. “PepTune: De Novo generation of therapeutic peptides with multi-objective-guided discrete diffusion”. In: (Dec. 2024). arXiv: 2412.17780 [q-bio.BM].
- [21] Xiaopeng Xu, Chencheng Xu, Wenjia He, Lesong Wei, Haoyang Li, Juexiao Zhou, Ruochi Zhang, Yu Wang, Yuanpeng Xiong, and Xin Gao. “HELM-GPT: de novo macrocyclic peptide design using generative pre-trained transformer”. In: *Bioinformatics* 40.6 (June 2024), btae364. ISSN: 1367-4811. DOI: 10.1093/bioinformatics/btae364. eprint: <https://academic.oup.com/bioinformatics/article-pdf/40/6/btae364/58585524/btae364.pdf>. URL: <https://doi.org/10.1093/bioinformatics/btae364>.
- [22] Aayush Shah, Chakradhar Guntuboina, and Amir Barati Farimani. “Peptide-GPT: Generative design of peptides using generative pre-trained transformers and bio-informatic supervision”. In: (Oct. 2024). arXiv: 2410.19222 [cs.LG].
- [23] Zhiwei Nie, Daixi Li, Yutian Liu, Fan Xu, Hongyu Zhang, Xiansong Huang, Xudong Liu, Zhennan Wang, Yiming Ma, Yuxin Ye, Feng Yin, Wen-Bin Zhang, Zhixiang Ren, Zhihong Liu, Zigang Li, and Jie Chen. “A unified peptide generative framework via a weakly order-dependent autoregressive language model and lifelong learning”. en. In: *J. Chem. Inf. Model.* 65.15 (Aug. 2025), pp. 7919–7935.
- [24] Ruheng Wang, Hang Zhang, Trieu Nguyen, Shasha Feng, Hao-Wei Pang, Xiang Yu, Li Xiao, and Peter Zhiping Zhang. “PepThink-R1: LLM for Interpretable Cyclic Peptide Optimization with CoT SFT and Reinforcement Learning”. In: (Aug. 2025). arXiv: 2508.14765 [cs.LG].
- [25] Stephen A Rettie, Katelyn V Campbell, Asim K Bera, Alex Kang, Simon Kozlov, Joshmyn De La Cruz, Victor Adebomi, Guangfeng Zhou, Frank DiMaio, Sergey Ovchinnikov, and Gaurav Bhardwaj. “Cyclic peptide structure prediction and design using AlphaFold”. en. Feb. 2023.
- [26] John Jumper, Richard Evans, Alexander Pritzel, Tim Green, Michael Figurnov, Olaf Ronneberger, Kathryn Tunyasuvunakool, Russ Bates, Augustin Židek, Anna Potapenko, Alex Bridgland, Clemens Meyer, Simon A A Kohl, Andrew J Ballard, Andrew Cowie, Bernardino Romera-Paredes, Stanislav Nikolov, Rishub Jain, Jonas Adler, Trevor Back, Stig Petersen, David Reiman, Ellen Clancy, Michal Zielinski, Martin Steinegger, Michalina Pacholska, Tamas Berghammer, Sebastian Bodenstein, David Silver, Oriol Vinyals, Andrew W Senior, Koray Kavukcuoglu, Pushmeet Kohli, and Demis Hassabis. “Highly accurate protein structure prediction with AlphaFold”. en. In: *Nature* 596.7873 (Aug. 2021), pp. 583–589.
- [27] Martin Pacesa, Lennart Nickel, Christian Schellhaas, Joseph Schmidt, Ekaterina Pyatova, Lucas Kissling, Patrick Barendse, Jagrity Choudhury, Srajan Kapoor, Ana Alcaraz-Serna, Yehlin Cho, Kourosh H Ghamary, Laura Vinué, Brahm J Yachnin, Andrew M Wollacott, Stephen Buckley, Adrie H Westphal, Simon Lindhoud, Sandrine Georgeon, Casper A Goverde, Georgios N Hatzopoulos, Pierre Gönczy, Yannick D Muller, Gerald Schwank, Daan C Swarts, Alex J Vecchio, Bernard L Schneider, Sergey Ovchinnikov, and Bruno E Correia. “One-shot design of functional protein binders with BindCraft”. en. In: *Nature* 646.8084 (Oct. 2025), pp. 483–492.

- [28] Richard Evans, Michael O’Neill, Alexander Pritzel, Natasha Antropova, Andrew Senior, Tim Green, Augustin Židek, Russ Bates, Sam Blackwell, Jason Yim, Olaf Ronneberger, Sebastian Bodenstern, Michal Zielinski, Alex Bridgland, Anna Potapenko, Andrew Cowie, Kathryn Tunyasuvunakool, Rishub Jain, Ellen Clancy, Pushmeet Kohli, John Jumper, and Demis Hassabis. “Protein complex prediction with AlphaFold-Multimer”. Oct. 2021.
- [29] J Dauparas, I Anishchenko, N Bennett, H Bai, R J Ragotte, L F Milles, B I M Wicky, A Courbet, R J de Haas, N Bethel, P J Y Leung, T F Huddy, S Pellock, D Tischer, F Chan, B Koepnick, H Nguyen, A Kang, B Sankaran, A K Bera, N P King, and D Baker. “Robust deep learning-based protein sequence design using ProteinMPNN”. en. In: *Science* 378.6615 (Oct. 2022), pp. 49–56.
- [30] Casper A Goverde, Martin Pacesa, Nicolas Goldbach, Lars J Dornfeld, Petra E M Balbi, Sandrine Georgeon, Stéphane Rosset, Srajan Kapoor, Jagrity Choudhury, Justas Dauparas, Christian Schellhaas, Simon Kozlov, David Baker, Sergey Ovchinnikov, Alex J Vecchio, and Bruno E Correia. “Computational design of soluble and functional membrane protein analogues”. en. In: *Nature* 631.8020 (July 2024), pp. 449–458.
- [31] Rohit Batra, Troy D Loeffler, Henry Chan, Srilok Srinivasan, Honggang Cui, Ivan V Korendovych, Vikas Nanda, Liam C Palmer, Lee A Solomon, H Christopher Fry, and Subramanian K R S Sankaranarayanan. “Machine learning overcomes human bias in the discovery of self-assembling peptides”. en. In: *Nat. Chem.* 14.12 (Dec. 2022), pp. 1427–1435.
- [32] Huitian Lin, Cheng Zhu, Tianfeng Shang, Ning Zhu, Kang Lin, Chengyun Zhang, Xiang Shao, Xudong Wang, and Hongliang Duan. “HighPlay: Cyclic peptide sequence design based on reinforcement learning and protein structure prediction”. en. In: *J. Med. Chem.* 68.11 (June 2025), pp. 12047–12057.
- [33] Michael A Siani, David Weininger, and Jeffrey M Blaney. “CHUCKLES: A method for representing and searching peptide and peptoid sequences on both monomer and atomic levels”. en. In: *J. Chem. Inf. Comput. Sci.* 34.3 (May 1994), pp. 588–593.
- [34] Kosala N Amarasinghe, Leonardo De Maria, Christian Tyrchan, Leif A Eriksson, Jens Sadowski, and Dušan Petrović. “Virtual screening expands the non-natural amino acid palette for peptide optimization”. en. In: *J. Chem. Inf. Model.* 62.12 (June 2022), pp. 2999–3007.
- [35] Jacob Devlin, Ming-Wei Chang, Kenton Lee, and Kristina Toutanova. In: *Proceedings of the 2019 Conference of the North*. Minneapolis, Minnesota: Association for Computational Linguistics, 2019.
- [36] Richard S. Sutton, David McAllester, Satinder Singh, and Yishay Mansour. “Policy Gradient Methods for Reinforcement Learning with Function Approximation”. In: *Advances in Neural Information Processing Systems 12 (NIPS 1999)*. Denver, CO, 1999, pp. 1057–1063.
- [37] Xiaolei Zhuang, Stephen J Stahl, Norman R Watts, Michael A DiMattia, Alasdair C Steven, and Paul T Wingfield. “A cell-penetrating antibody fragment against HIV-1 Rev has high antiviral activity: characterization of the paratope”. en. In: *J. Biol. Chem.* 289.29 (July 2014), pp. 20222–20233.
- [38] Hao Wu, Guillaume Mousseau, Sonia Mediouni, Susana T Valente, and Thomas Kodadek. “Cell-permeable peptides containing cycloalanine residues”. In: *Angew. Chem. Int. Ed Engl.* 55.41 (Oct. 2016), pp. 12637–12642.
- [39] Jiajun Yu, Yizhen Zheng, Huan Yee Koh, Shirui Pan, Tianyue Wang, and Haishuai Wang. “Collaborative expert LLMs guided multi-objective molecular optimization”. In: (Mar. 2025). arXiv: 2503.03503 [q-bio.BM].
- [40] Hyomin Kim, Yunhui Jang, and Sungsoo Ahn. “MT-Mol: Multi agent system with tool-based reasoning for molecular optimization”. In: (May 2025). arXiv: 2505.20820 [cs.AI].

## Supplementary Information

### S1. Example of Masking Strategies

To illustrate how the masking strategies described in Section 2.5 work in practice, consider the peptide sequence  $p = "r_1|r_2|r_3|r_4|r_5"$ , where the positions selected for optimization are  $O = \{2, 3, 4\}$ , giving  $|O| = 3$  input contexts.

#### Single-agent Mode

Under the self-mask strategy, each context masks only the position being optimized:

$$\text{agent} \leftarrow "r_1|?|r_3|r_4|r_5", \quad \text{agent} \leftarrow "r_1|r_2|?|r_4|r_5", \quad \text{agent} \leftarrow "r_1|r_2|r_3|?|r_5".$$

In contrast, the neighbor-mask strategy masks neighboring positions around the target position, producing:

$$\text{agent} \leftarrow "r_1|r_2|?|?|r_5", \quad \text{agent} \leftarrow "r_1|?|r_3|?|r_5", \quad \text{agent} \leftarrow "r_1|?|?|r_4|r_5".$$

#### Multi-agent Mode

Under the self-mask strategy, each context masks only the position being optimized, and each context is handled by a corresponding agent:

$$\text{agent}_2 \leftarrow "r_1|?|r_3|r_4|r_5", \quad \text{agent}_3 \leftarrow "r_1|r_2|?|r_4|r_5", \quad \text{agent}_4 \leftarrow "r_1|r_2|r_3|?|r_5".$$

In contrast, the neighbor-mask strategy masks neighboring positions around the target position, and each context is handled by a corresponding agent:

$$\text{agent}_2 \leftarrow "r_1|r_2|?|?|r_5", \quad \text{agent}_3 \leftarrow "r_1|?|r_3|?|r_5", \quad \text{agent}_4 \leftarrow "r_1|?|?|r_4|r_5".$$

### S2. Score Analysis and Model Collapse Behavior

It is important to note that in Figure 8, the mean score is computed as the sum of all unique peptide scores divided by the number of unique peptides, consistent with the original PepINVENT method. This approach is valid only when the uniqueness of generated peptides remains close to 100%. In certain PepEVOLVE configurations, we observed a decline in peptide uniqueness over training steps. To address this, we conducted a refined analysis of score progression by calculating the mean score based on all generated peptides, rather than only the unique ones.

By doing this, we observe pronounced fluctuations after approximately 400 steps in both cases involving self-mask context visibility, as illustrated in Figure 11. We interpret this as evidence of model collapse, which appears to arise from two interacting factors. First, the group-relative advantage mechanism tends to overemphasize certain score components, effectively oversquashing the optimization signal. Second, within the self-mask context, the model generates only a single monomer at a time. This setting involves significantly fewer tokens than the neighbor-mask context, which requires roughly three times as many tokens for generation. The limited token context amplifies the oversquashing effect, reducing learning diversity and ultimately leading to model collapse. Moreover, because group-relative advantage normalizes rewards across all peptides in a group, even high-quality peptides may be penalized if others in the group achieve better scores. Over time, this causes the model to converge toward a narrow subset of “top-tier” peptides, reducing variability and leading to the generation of fewer unique sequences. The observed fluctuations between very high and very low scores can be further explained by differences in the optimization landscapes across input contexts. Some contexts experience collapse, while others remain stable. In collapsed contexts, the model produces only a small number of unique peptides, resulting in lower aggregate scores, not because the generated peptides themselves are of poor quality, but because the score normalization is based on the total number of generated samples.

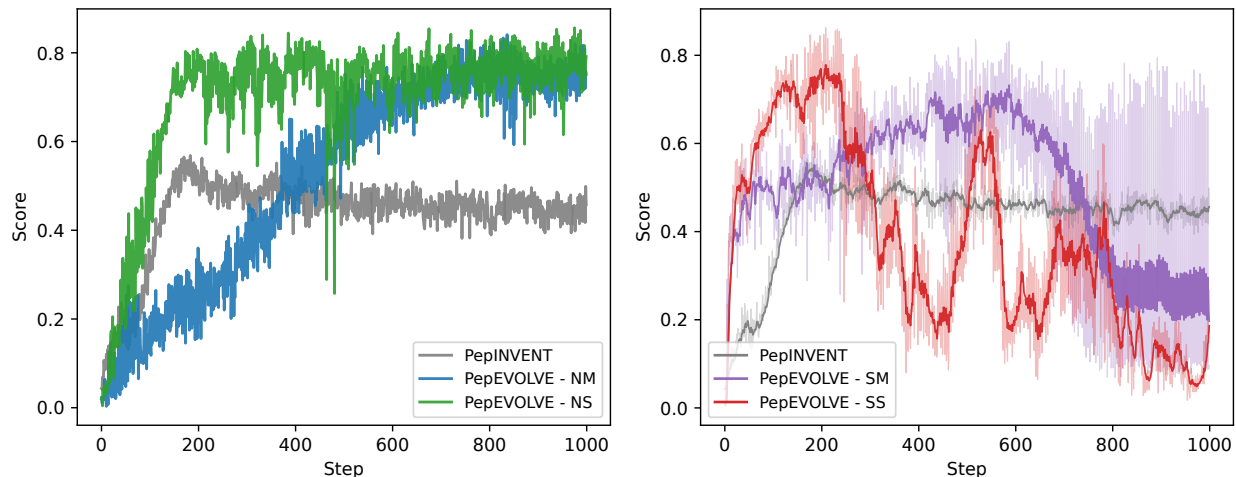


Figure 11: **Generated peptide scores over steps when the mean score is calculated using all generated peptides rather than only unique ones.** Left: Comparison between PepINVENT and PepEVOLVE (neighbor-mask) configurations. Right: Comparison between PepINVENT and PepEVOLVE (self-mask) configurations, shown with exponential moving average smoothing.

This relationship is further illustrated in Figure 9. The self-mask context produces fewer unique peptides overall, but among the peptides with scores between 0.9 and 1.0, it actually performs better than all other contexts. This matches our earlier explanation: as the model collapses, only the very best peptides remain.

Nevertheless, all four configurations of PepEVOLVE still outperform PepINVENT in producing optimized peptides. Notably, PepINVENT fails to generate any peptides with a score above 0.8, whereas PepEVOLVE generates a significantly higher portion of peptides with a score above 0.8